GPS Signal Tracking and Positioning through Long Duration Wide Band Interference with Multiple Model Kalman Filter

Wengxiang Zhao, *Illinois Institute of Technology*
Samer Khanafseh, *Illinois Institute of Technology*
Boris Pervan, *Illinois Institute of Technology*

BIOGRAPHY

Wengxiang Zhao received the bachelor's degree in mechanical engineering from Huazhong University of Science and Technology, Wuhan, China, in 2016. He is working toward the Ph.D. degree in the Navigation Laboratory, Department of Mechanical and Aerospace Engineering, Illinois Institute of Technology (IIT) in Chicago, Chicago, IL, USA.

Samer Khanafseh received the M.Sc. and Ph.D. degrees in aerospace engineering from the Illinois Institute of Technology (IIT), Chicago, IL, USA, in 2003 and 2008, respectively. He is currently a Research Associate Professor with IIT. His research interests include high-accuracy and high-integrity navigation algorithms, cycle ambiguity resolution, high-integrity applications, fault monitoring, and robust estimation techniques.

Boris Pervan received the B.S. degree from the University of Notre Dame, Notre Dame, Indiana in 1986, the M.S. degree from the California Institute of Technology, Pasadena, CA, USA in 1987, and the Ph.D. degree from Stanford University, Stanford, CA, USA in 1996. He is currently a Professor of Mechanical and Aerospace Engineering at IIT.

ABSTRACT

In this paper, we extend prior research on Multiple Model (MM) Kalman filtering for Global Positioning System (GPS) carrier phase and frequency estimation in weak or jammed signal scenarios. MM Kalman filtering enables GPS receivers to maintain high-quality positioning, navigation, and timing solutions even during prolonged jamming periods, lasting up to several hours.

In prior research, we demonstrated the superior tracking performance of the MM Kalman filter over traditional Phase Lock Loop (PLL) under strong Radio Frequency Interference (RFI) event scenario. The tracking result was validated for a single satellite under a 15 dB-Hz carrier to noise ratio (C/N_0). In this research, we continue the work to obtain position solutions based on the MM Kalman filter estimation output when all satellites are being jammed by wideband radio frequency interference.

We further enhance performance by augmenting the MM Kalman filter with historical navigation data knowledge and implementing an upload-robust bit prediction strategy to support extended operational duration. A detection method based on IODE (Issue of Data, Ephemeris) bits is introduced and applied to enhance performance during periods when the navigation message remains unchanged.

With these methods, GPS receivers are shown to be able to operate through long duration wideband jamming events and provide high quality positioning solutions.

I. INTRODUCTION

Normally, Global Positioning System (GPS) receivers use Phase Lock Loops (PLL) for carrier phase tracking. A PLL uses a phase discriminator and loop filter to continuously measure and compensate for the phase difference between the local signal replica and the incoming carrier signal. During a Radio Frequency Interference (RFI) event, the additive noise pumped into the PLL degrades the phase discriminator's ability to measure the true carrier phase, which in turn causes accumulated error in carrier reconstruction and eventually loss of phase lock. Typical methods for PLL tracking of weak signals include extending coherent averaging times (T_{co}) and tightening noise bandwidths.

Using large values of T_{co}, for example greater than 20 ms for Global Positioning System (GPS) signals, means integrating in-phase (I) and quadrature (Q) signal samples across navigation data bit transitions. Existing techniques to extend averaging time over multiple data bits, such as non-coherent memory discriminators Borio and Lachapelle (2009) and real-time bit estimation techniques Stevanovic and Pervan (2017), introduce biases in the discriminator output in the presence of strong RFI that lead, in turn, to biases in the reconstructed carrier frequency and ultimately loss of phase lock. Tightening the noise bandwidth can

be effective in reducing the tracking error variance, given a linear classic control PLL model, but it does not help to reduce the discriminator output variance Stevanovic and Pervan (2017). In the presence of strong RFI the discriminator output can saturate, making the PLL nonlinear and leading to instability and loss of lock.

The PLL is fundamentally a feedback control system, where the I and Q samples, as interpreted by the discriminator, serve as the sensor (measurement) and the loop filter as the compensator (controller). However, the feedback control model is not the only way to approach the carrier tracking problem. As first proposed in Psiaki and Jung (2002) and advocated more recently in Vila-Valls et al. (2017) it can also be understood as an estimation problem amenable to Kalman filtering.

Kalman filter implementations are more flexible than PLLs because their component dynamic and measurement models can be designed to suit the needs of specific implementation scenarios. They are also optimal estimators for applications with Gaussian input noise, which is the case for wideband RFI. In earlier work, Kalman filters were used to estimate carrier phase through ionospheric scintillation with $T_{av} < 20$ ms in (Vila-Valls et al., 2015) and (Humphreys et al., 2010) in simulation tests and in (Humphreys et al., 2005) and (Vila-Valls et al., 2020) with some limited experiments. A Kalman filter architecture was also used in (Psiaki and Jung, 2002) with to track numerically simulated weak GPS signals.

A major challenge in using a Kalman filter for GNSS carrier phase 'tracking' is that it is a hybrid stochastic estimation problem, requiring simultaneous estimation of discrete navigation data bits and continuous carrier phase. In the case where data bits are completely unknown, (Psiaki and Jung, 2002) addressed bit transition using a Bayesian bit estimation technique where equal a-priori probability was assumed for each new data bit.

The applications we are initially targeting are aviation operations threatened by unpredictable wideband RFI events. There is no reliable means today to supply navigation data bits from an external source to aircraft or related ground based GNSS augmentation systems. We do not address the problem of signal acquisition during interference because our goal is to continue tracking of existing satellites through RFI events of limited duration, not to start up and operate continuously in low signal strength environments (e.g., indoors with A-GNSS). However, we do leverage the fact that broadcast ephemerides decoded prior to the onset of RFI, except for events of especially long duration, will still be valid for satellite position and clock determination during the event, in the case of GPS for at least two hours.(Dunn, 2013)

Utilizing previously decoded navigation data properly and maintaining awareness of any ephemeris cutovers and uploads can significantly improve tracking and estimation performance. In this case, the receiver must obtain new data whenever there is an ephemeris cutover or new navigation data upload, which in the case of Global Positioning System (GPS) operations, can happen at any time. Understanding that navigation data changes happen infrequently for GPS, we then introduce a detection method for such changes to enable adaptive updates of a-priori bit probabilities when needed, while at the same time maximizing the use of data bit knowledge in cases where a navigation data transition has not occurred.

In our prior work in (Zhao and Pervan, 2019), we carried out preliminary simulation trials to study the feasibility of a Multiple Model (MM) Kalman filter approach to carrier phase estimation, with encouraging results for static phase and different levels of knowledge of the navigation data bits. In (Zhao and Pervan, 2020b), we showed experimental results under interference-free conditions. The MM filter was able to generate the same carrier phase estimates as the PLL in nominal signal strength scenarios. In (Zhao and Pervan, 2020a), we performed experiments under interference with results showing superior performance of the MM filter over the PLL.

In Section II of this paper, the MM algorithm and the Kalman filter components are reviewed. Section III describes the upload-robust bit prediction strategy and IODE check detection method. Section IV describes the experimental scenario and setup. Section V presents positioning results under normal and interference conditions. Section VI, we summarize the results and share ideas for future research.

II. KALMAN FILTER AND MM ALGORITHM

While PLLs are typically fixed structures with predefined discriminators and loop filters, Kalman filters have internal adaptability to rely more heavily on either measurements or phase dynamics depending on the noise levels. Wideband interference events contribute additive white Gaussian noise (AWGN) directly into the I and Q measurements. For typical PLL implementations using phase discriminators, these noisy measurements can easily cause phase errors to exceed the pull-in limit of the discriminator, which usually leads to cycle slips and eventual loss of lock.

The shortcomings of a traditional PLL can be overcome using a Kalman filter to estimate the carrier frequency and phase directly. The goal in carrier tracking is to produce the best phase and frequency estimates under noisy conditions, which the Kalman filter can optimally accomplish given that the noise is white (which is the case for wideband interference). Figure 1 shows a top-level block diagram of an IMM/Kalman-based carrier phase tracking architecture as it would be implemented in a software defined receiver (SDR).

In our interference scenario, we assume that the receiver is already tracking, post-acquisition, before being subjected to an RFI

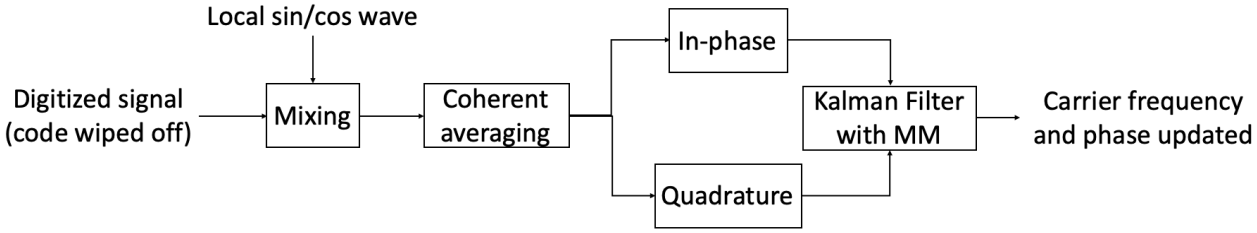

Figure 1: Top-level view of MM/Kalman-based carrier phase estimation in an SDR

event, and as a result, the Kalman filter estimate error is small immediately prior to the event onset.

1. Dynamic Model

Our goal is to estimate the carrier phase and frequency in real time. Over one pre-detection averaging interval, T_{av}, the total phase change is $\phi_{tot} = \phi_{Dopp} + \phi_{clk}$, where ϕ_{Dopp} is the phase change due to relative movement between the satellite and receiver. For our current development, we assume a static receiver, e.g., a Ground Based Augmentation System (GBAS) reference receiver, so that ϕ_{Dopp} is the result of satellite motion only, which is known and removed using the last decoded broadcast ephemeris. (In future work, user motion will be accounted for using inertial sensors.) Therefore, we only need a clock phase dynamic model for our Kalman filter. The Power Spectral Density (PSD) for clock phase noise can be expressed using the conventional power law model

$$S(f) = \frac{f_0^2}{f^2}(h_2 f^0 + h_1 f^{-1} + h_0 f^{-2} + h_{-1} f^{-3} + h_{-2} f^{-4}). \tag{1}$$

The values of the h coefficients will depend on the specific receiver and satellite clocks. Example coefficients for a TCXO clock are $h_2 = 0,\ h_1 = 0,\ h_0 = 4.9639 \times 10^{-3},\ h_{-1} = 0,\ h_{-2} = 7.4458 \times 10^{-6}$.

For Kalman filter implementation, we define a state vector to include signal amplitude (A), clock phase (ϕ_{clk}), and clock frequency (f_{clk}), and a dynamic process model,

$$\begin{bmatrix} A \\ \phi_{clk} \\ f_{clk} \end{bmatrix}_{k+1} = \begin{bmatrix} 1 & 0 & 0 \\ 0 & 1 & \Delta t \\ 0 & 0 & 1 \end{bmatrix} \begin{bmatrix} A \\ \phi_{clk} \\ f_{clk} \end{bmatrix}_k + w_k \tag{2}$$

where $\Delta t = T_{av}$ is the time increment represented by index k, and $w_k \sim N(0, W)$ is time independent white noise. The process noise covariance matrix is (Chan et al., 2014)

$$W = \begin{bmatrix} \delta^2 & 0 & 0 \\ 0 & S_f \Delta t + \frac{S_g \Delta t^3}{3} & \frac{S_g \Delta t^2}{2} \\ 0 & \frac{S_g \Delta t^2}{2} & \frac{S_f}{\Delta t} + \frac{4}{3} S_g \Delta t \end{bmatrix} \tag{3}$$

where

$$S_g = 2\pi^2 h_{-2} \tag{4}$$

and

$$S_f = \frac{h_0}{2}. \tag{5}$$

f_0 is the carrier frequency (e.g., $f_0 = f_{L1} = 1575.42$ MHz for the GPS L1 signal), and $\delta^2 \approx 0$ is included to allow for small nominal process noise on the amplitude state.

2. Measurement Model

The measurement model, with the known contributions of ϕ_{Dopp} to the in-phase and quadrature components removed, is

$$I_k = d_k A_k \cos(\phi_{clk,k}) + v_{i,k} \tag{6}$$

$$Q_k = d_k A_k \sin(\phi_{clk,k}) + v_{q,k} \tag{7}$$

where $d_k = \pm 1$ is the navigation data bit and $v_{i,k}$ and $v_{q,k}$ are white measurement processes distributed as $[v_{i,k}\ v_{q,k}]^T \sim N(0, V_k)$ with $V = I\sigma^2_{v,k}$. The measurement error variance $\sigma^2_{v,k}$ for a unit amplitude signal is related to the carrier-to-noise ratio ($C/N_{0,k}$) by

$$C/N_{0,k} = 10^{\frac{C/N_{0,k}\,[\text{dBHz}]}{10}} \tag{8}$$

$$\sigma^2_{v,k} = \frac{1}{2T_{av}C/N_{0,k}} \tag{9}$$

The observation equations 6 and 7 are nonlinear in state $\phi_{clk,k}$, so to execute the Kalman measurement update they must be linearized about the best available estimate, $\hat{\phi}_{clk,k|k-1}$, obtained from the previous dynamic update.

3. MM Algorithm

The MM algorithm is a dynamic multiple hypothesis estimator. It assumes the system obeys one of a finite number of continuous models at a time but is capable of switching between models at discrete intervals. The algorithm is described comprehensively in (Bar-Shalom et al., 2004), so only a brief summary will be given here and with emphasis on application to the problem at hand—GNSS data bit transitions.

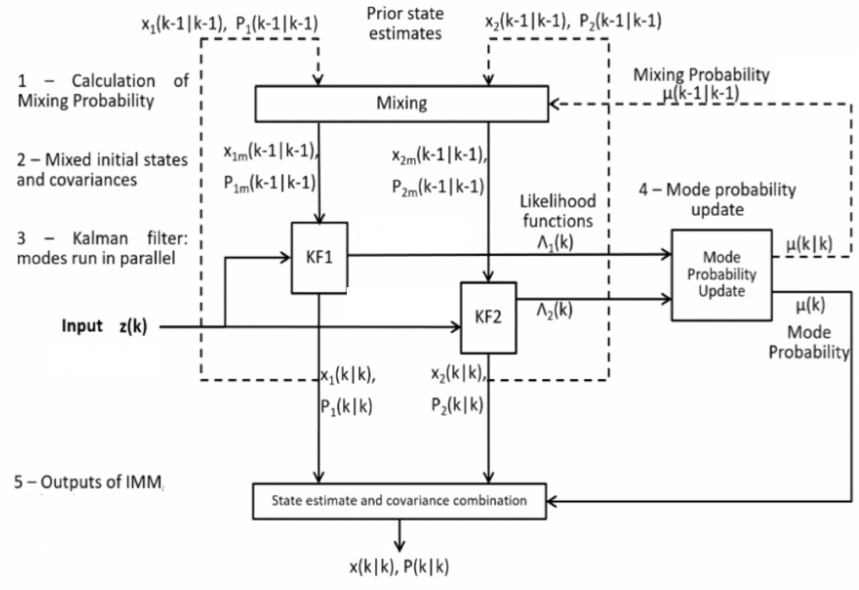

Figure 2: The MM algorithm

A flowchart of an example two-hypothesis MM estimator is shown in Figure 2. At the top, prior state estimate vectors

$x_1(k-1|k-1)$ and $x_2(k-1|k-1)$ and their corresponding error covariance matrices $P_1(k-1|k-1)$ and $P_2(k-1|k-1)$ are obtained from two component Kalman filters executed in the previous cycle. These are input into a "mixing" function to compute modified inputs for the next Kalman filter cycle: $x_{1m}(k-1|k-1)$, $P_{1m}(k-1|k-1)$ and $x_{2m}(k-1|k-1)$, $P_{2m}(k-1|k-1)$. Each Kalman filter represents a specific mode, which may differ from the other in the dynamic model or measurement model (or both). Each filter, using its own measurement model, will then perform a measurement update using the same measurement $z(k)$ and a time update with its own dynamic model. Likelihood functions $\Lambda_1(k)$ and $\Lambda_2(k)$ are then evaluated and used to calculate current mode-state (μ_k) and mixing ($\mu_{k|k}$) probabilities, the latter used to commence the next cycle. The Appendix provides additional detail. The output state estimate vector and error covariance matrix $x(k|k)$ and $P(k|k)$ are computed using the individual Kalman filter results $x_1(k|k)$, $P_1(k|k)$, and $x_2(k|k)$, $P_2(k|k)$ and the mode probability vector μ_k.

In our MM application, two modes run in parallel as shown in Figure 3, corresponding to two measurement models with navigation data bit values $d = 1$ and $d = -1$. The Kalman measurement updates for both modes are performed using the same I and Q measurements. The dynamic models are also the same for both modes, as defined in Section II.1.

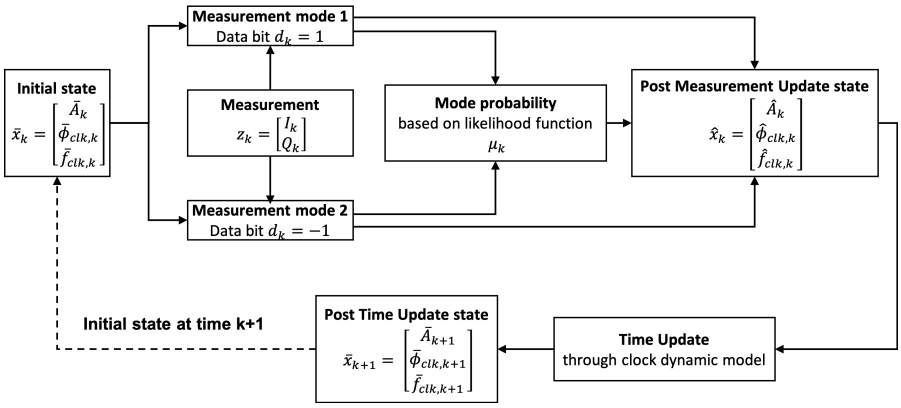

Figure 3: MM algorithm in our case

For now, we assume the data bits to be sequentially independent, the mode (bit) transition probabilities are both $\frac{1}{2}$, and the mode transition matrix is a 2×2 matrix with each element equal to $\frac{1}{2}$. The "mixing" process shown in Figure 2 for the standard MM algorithm is not needed in this case because of the uniform structure of the mode transition probability matrix. However, the MM can also accommodate more general cases, where there is reduced uncertainty in bit transitions, as will be discussed in Section III.

III. NAVIGATION DATA BIT PREDICTION

Navigation data messages are standardized, well-structured binary bits broadcast by the satellites to communicate with GPS receivers about ephemerides, almanacs, satellite health status, and other information. For this work, we focus only on the GPS L1 signal and its 'legacy' navigation (LNAV) data bits. The navigation data message is modulated on the carrier at 50 bps and contains 5 sub-frames, each of which has 300 bits, and each bit is 20 ms in length. Sub-frames 4 and 5 each have 25 separate pages. Every 30 seconds GPS satellites will transmit one frame: 1500 bits including sub-frames 1, 2 and 3 and one page each from sub-frame 4 and 5. Thus, collection of the whole navigation data message (superframe) takes at least 12.5 minutes. The navigation data bit structures are pre-defined in IS-GPS-200H (Dunn, 2013).

1. Upload-robust Data Bit Prediction Strategy

We consider the case where a receiver decodes enough sub-frames before RFI onset to enable partial data bit prediction during the event. Using navigation data bits collected over several days, we have categorized the bits that remain predictable through ephemeris cutovers and new uploads. Some bits never change (e.g., preamble bits) or are easily predictable (e.g., TOW and subframe ID bits). For a number of other parameters (e.g., related with SV clock corrections and certain orbit elements), the most significant bits do not change. Based on the information gained from the collected data, we have developed a partial bit prediction strategy to predict only the bits that remain unchanged through navigation data uploads. The strategy is conservative most of the time because a larger number of bits would remain predictable even through ephemeris cutovers, but it is necessary to ensure tracking continuity through uploads, which can happen at any time.

Figure 4 shows example data bit prediction maps for the upcoming 5 sub-frames based on the last 5 sub-frames. The data bits

from the last 5 sub-frames (50 rows $\times$ 30 columns = 1500 bits in total, each block representing one data bit) are shown on the left. The bits predictable through a subsequent upload are shown on the right. Dark blue blocks represent bit '$d = 1$', light blue for bit '$d = -1$', and unpredictable bits are in grey. For predictable bits, we use a prior probability of 1 in the MM estimator; for bits deemed unpredictable, we use a prior probability of $1/2$.

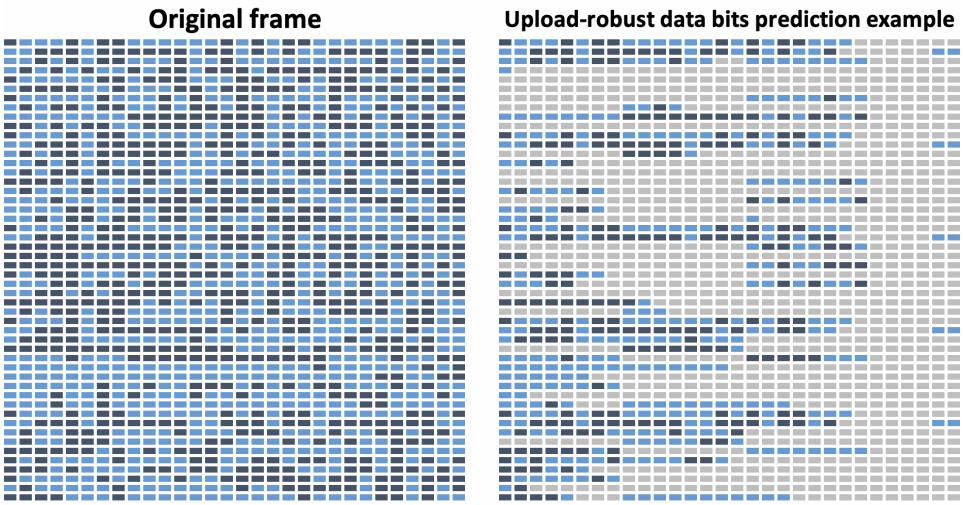

Figure 4: Data bit prediction example

The figure provides a rough visual idea of how many data bits are predictable. Using this bit prediction strategy, an average of approximately 38% of bits are predicable over the entire set of 25 frames.

2. IODE Check

As navigation data uploads can occur at any time, we can only predict a limited portion of the navigation data. Attempting to predict an extensive segment might result in the loss of tracking continuity due to the potential large number of incorrectly predicted bits. Nevertheless, if we can detect navigation data upload events as they happen, we can utilize all known data bits—achieving 100% prediction accuracy—between uploads.

IODE (Issue of Data, Ephemeris) bits offer users a convenient means to identify changes in the ephemeris representation parameters. The IODE is a string of 8 bits found in three locations: word 8 of sub-frame 1, word 3 of sub-frame 2, and word 10 of sub-frame 3. By comparing the IODE bits in a new block of sub-frames with those in the immediately preceding frame, any differences indicate the occurrence of either an ephemeris cutover or a navigation upload.

For each subframe we receive, we perform an IODE check against the previous IODE. If they are the same we assert that the navigation data has not changed and we move to a 100% bit prediction strategy for the rest of the navigation data bits.

Obviously, interference events tremendously increase the difficulty of correctly verifying whether the IODE bits have changed or not. To minimize the risk of losing continuity, considering redundant IODEs available in each block of five subframes of navigation data is crucial. One approach is to check all three IODEs from the current subframes 1, 2, and 3, ensuring they are identical, and then compare them with the IODEs in the previous frame.

There is minimal downside in "detecting" a navigation data change when none actually occurred, as the data bit prediction strategy can simply remain in upload-robust mode. However, the reverse is not true. If a new navigation data upload goes undetected, and we transition to 100% prediction mode, continuity loss can be expected.

IV. EXPERIMENTAL SCENARIO AND SETUP

We use a SKYDEL simulation engine to generate GPS L1 C/A RF signal and save the I, Q data into a file for post processing. The sampling rate is 12.5 MHz and intermediate frequency set to 0 Hz. Then we use a Software Defined Receiver (SDR) to post process the data. The MM Kalman filter estimator is implemented in the SDR.

The experiment involved a static GPS reference receiver operating over a 4 minute period with four satellites (PRN 1, 11, 28, 30). The true receiver location was $41°50'12.9264''$ N, $-87°37'38.2368''$ W, 2 meters height. We created a clean signal scenario (no interference) as a benchmark for positioning accuracy comparison. For the jamming signal scenarios, we added

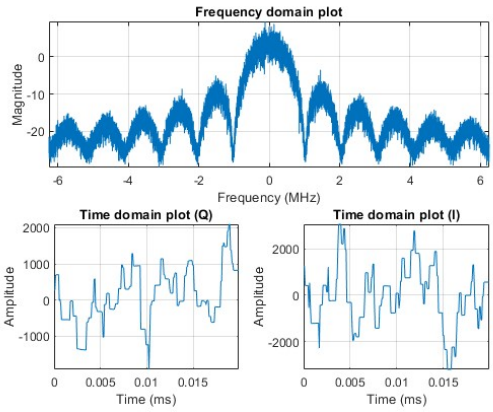

(a) Signal spectrum

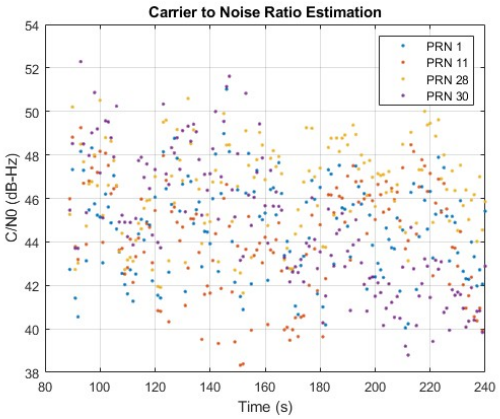

(b) C/N_0 estimation

Figure 5: Clean signal

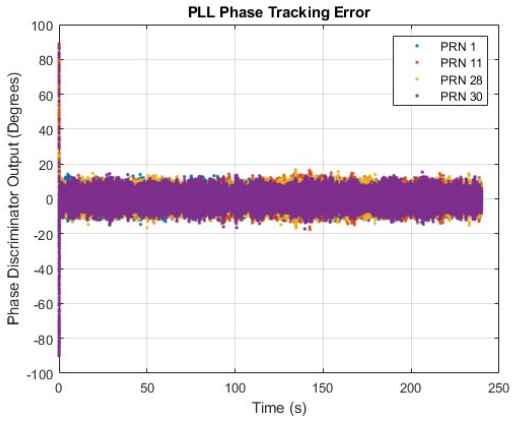

(a) Phase tracking error

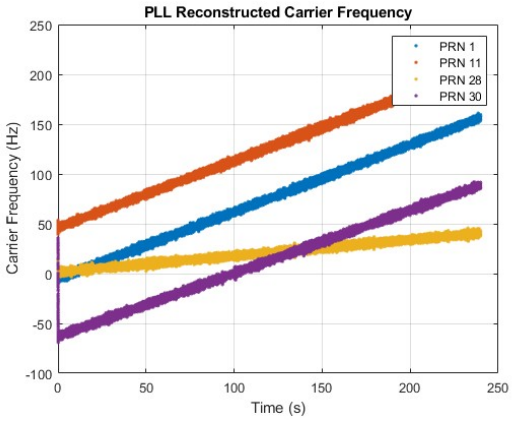

(b) Reconstructed carrier frequency

Figure 6: PLL output

wide band (8 MHz) AWGN noise onto the clean signal. The onset of the RFI event was 2 minutes after start so that the receiver had sufficient time for acquisition and to lock on to the nominal signals. This design is aligned jamming event scenario where a GBAS receiver is in normal operation and then abruptly subjected to RFI.

The carrier to noise ratio drops to approximately 15 dB-Hz for all four satellites during the jamming period. At 15 dB-Hz, the PLL is not able to maintain phase lock, so only the MM Kalman filter results will be presented for the jamming scenario.

V. MM KALMAN FILTER POSITIONING RESULT

Nominally the SDR uses a PLL aided Delay Lock Loop (DLL) architecture with coherent PLL tracking. Under jamming, the PLL will lose lock; thus in this scenario we instead use the carrier estimator output from the MM Kalman filter to feed the DLL.

1. No Interference Case

The clean signal spectrum is shown in Figure 5. After down converting to 0 Hz intermediate frequency, the signal has a clear peak at the center frequency with a sinc function shape due to the coherent averaging. Figure 5 shows that the carrier to noise ratio (C/N_0) for the clean signal is approximately 46 dB-Hz. Figure 6 shows the PLL phase tracking error and reconstructed carrier frequency.

Position solutions are shown in Figure 7. The final average position solution is $41°50'12.9516''$ N, $-87°37'38.2297''$ W, 2.5

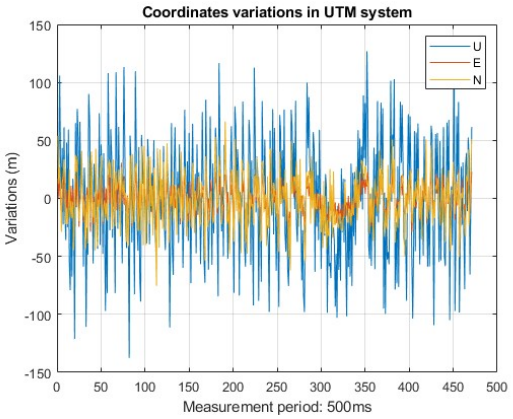

(a) ENU coordinates estimation

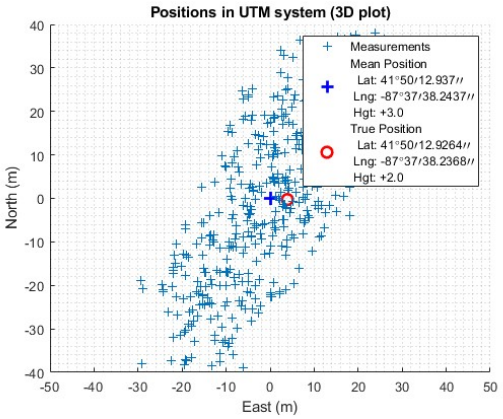

(b) Reconstructed carrier frequency

Figure 7: Position solution

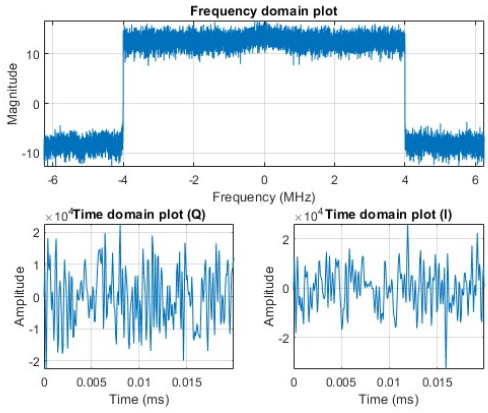

(a) Signal spectrum

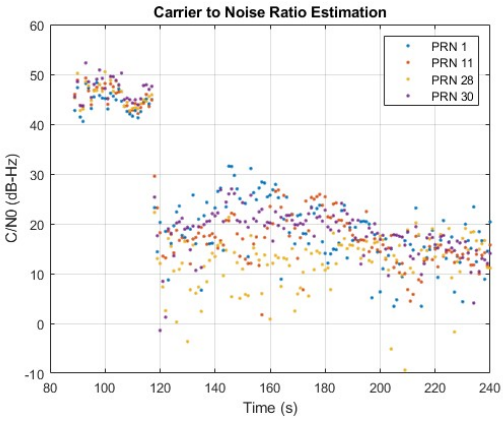

(b) C/N_0 estimation

Figure 8: Jammed signal

meters height, all close to the true location $41°50'12.9264''$ N, $-87°37'38.2368''$ W, 2 meters height. The mean error on East/North/Up directions are 3.9/0.2/0.5 meters with associated standard deviation of 13/23/50 meters.

2. Jamming Case

During the RFI event, the characteristics of the jammed signal are illustrated in Figure 8. The 8 MHz wideband RFI significantly overwhelms the signal power spectrum, causing the GPS L1 C/A signal to be buried beneath the noise. The C/N_0 estimation reveals a substantial decrease at 120 seconds, indicating the impact of the interference. The average C/N_0 value throughout the jamming period hovers around 15 dB-Hz.

The PLL has already lost lock under the jamming, as depicted in Figure 9. The PLL phase tracking error reaches 90 degrees, signifying that the phase discriminator is saturated by the noise and unable to provide any meaningful information about the carrier phase. Additionally, there is a substantial variance in the reconstructed carrier frequency, reaching up to 20 Hz.

The MM Kalman filter starts prior to the onset of interference and operates continuously throughout the jamming period. Figure 10 illustrates the clock phase estimation error and carrier frequency estimation error derived from the output of the MM Kalman filter. The average variance for the carrier frequency estimation error is 3 Hz. This precise carrier frequency estimation enables the DLL to generate accurate code measurements and high-quality position solutions. Figure 11 illustrates the final position solution obtained through the MM Kalman filter during a 15 dB-Hz jamming period. The variance in ENU coordinates slightly increases after the interference event begins. The averaging resulting position solution is $41°50'12.8692''$

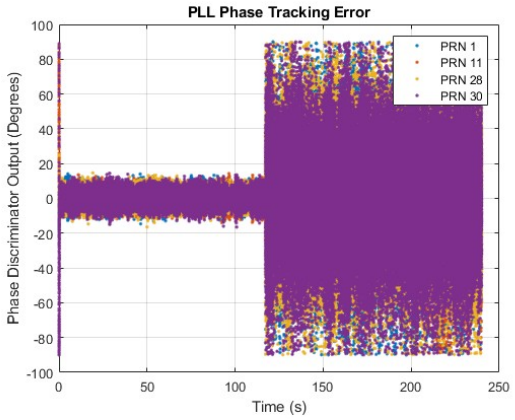

(a) Phase tracking error

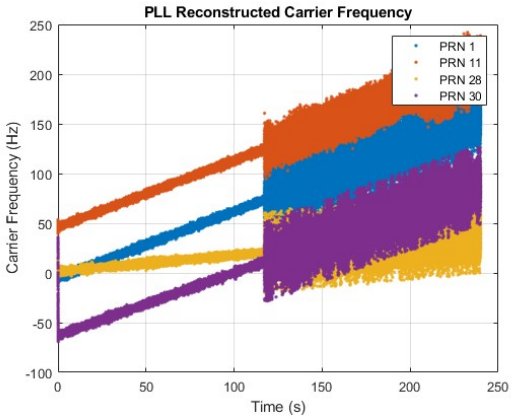

(b) Reconstructed carrier frequency

Figure 9: PLL output under jamming

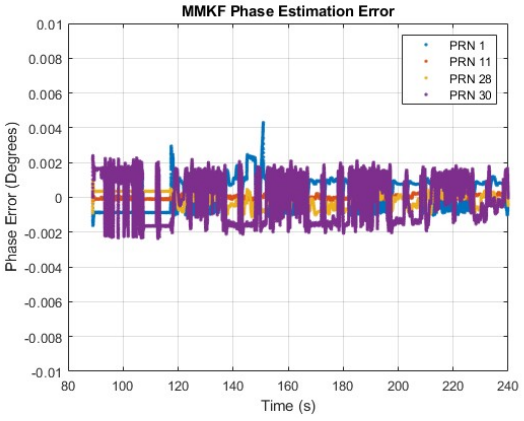

(a) Clock phase estimation error

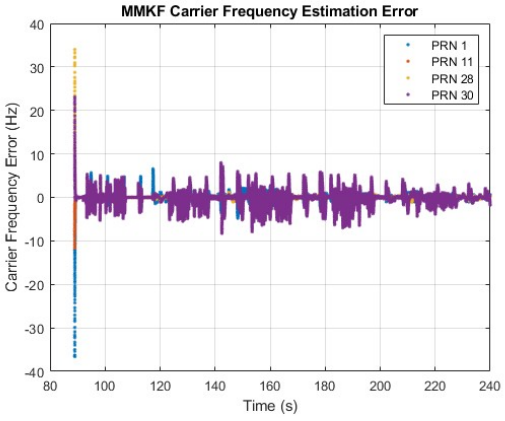

(b) Carrier frequency estimation error

Figure 10: MM Kalman filter output under jamming

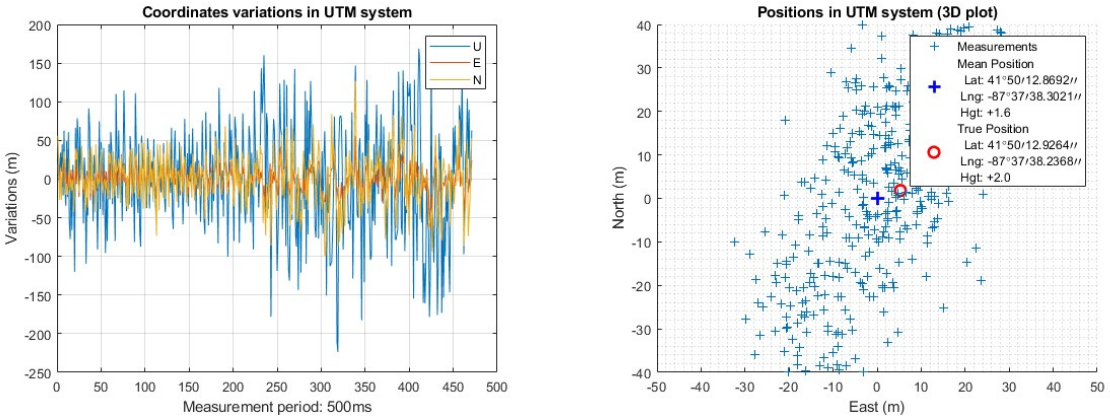

(a) ENU coordinates estimation

(b) Reconstructed carrier frequency

Figure 11: Position solution

N, $-87°37'38.3021''$ W, with a height of 1.6 meters. The true location is $41°50'12.9264''$ N, $-87°37'38.2368''$ W, and a height of 2 meters. The mean error on East/North/Up directions are 5/1.8/1.9 meters with associated standard deviation of 16/32/63 meters.

While the positioning accuracy is slightly worse than clean signal data, it is crucial to consider that this discrepancy occurred under a 15 dB-Hz jamming period. Additionally, it's noteworthy that the PLL loses lock immediately when jamming starts.

VI. CONCLUSION

In this research work, we enhance the performance of our MM Kalman filter estimation by effectively leveraging navigation data bit information. We introduce an upload-robust bit prediction strategy and a triple IODE check method to enable the MM Kalman filter to operate freely for an extended duration. We evaluate the positioning accuracy under a 15 dB-Hz jammed signal, and it is evident that the MM Kalman filter continues to produce high-quality position solutions even when all satellites are jammed.

ACKNOWLEDGEMENTS

We would like to thank our sponsors at the Federal Aviation Administration (FAA) for supporting this research. The views and opinions expressed in this paper are those of the authors and do not necessarily reflect those of any other organization or person.

REFERENCES

Bar-Shalom, Y., Li, X. R., and Kirubarajan, T. (2004). *Estimation with Applications to Tracking and Navigation: Theory, Algorithms, and Software*. John Wiley Sons.

Borio, D. and Lachapelle, G. (2009). A non-coherent architecture for GNSS digital tracking loops. *Annales Des Télécommunications*, 64(9-10):601–614.

Chan, F.-C., Joerger, M., and Pervan, B. (2014). Stochastic modeling of atomic receiver clock for high integrity gps navigation. *IEEE Transactions on Aerospace and Electronic Systems*, 50(3):1749–1764.

Dunn, M. J. (2013). Global Positioning System Directorate Systems Engineering & Integration: Interface Specification IS-GPS-200.

Humphreys, T. E., Psiaki, M. L., and Kintner, P. M. (2010). Modeling the Effects of Ionospheric Scintillation on GPS Carrier Phase Tracking. *IEEE Transactions on Aerospace and Electronic Systems*, 46(4):1624–1637.

Humphreys, T. E., Psiaki, M. L., Kintner, P. M., and Ledvina, B. M. (2005). GPS Carrier Tracking Loop Performance in the presence of Ionospheric Scintillations. *Proceedings of the 18th International Technical Meeting of the Satellite Division of The Institute of Navigation (ION GNSS 2005)*, pages 156–167.

Psiaki, M. L. and Jung, H. Y. (2002). Extended Kalman filter methods for tracking weak GPS signals. *Proceedings of the 15th International Technical Meeting of the Satellite Division of The Institute of Navigation (ION GPS 2002)*, pages 2539–2553.

Stevanovic, S. and Pervan, B. (2017). Coasting Through Wideband Interference Events using Robust Carrier Phase Tracking. *Proceedings of the Satellite Division's International Technical Meeting*.

Vila-Valls, J., Closas, P., and Fernandez-Prades, C. (2015). Advanced KF-based methods for GNSS carrier tracking and ionospheric scintillation mitigation. *2015 IEEE Aerospace Conference*.

Vila-Valls, J., Closas, P., Navarro, M., and Fernandez-Prades, C. (2017). Are PLLs dead? A tutorial on kalman filter-based techniques for digital carrier synchronization. *IEEE Aerospace and Electronic Systems Magazine*, 32(7):28–45.

Vila-Valls, J., Linty, N., Closas, P., Dovis, F., and Curran, J. T. (2020). Survey on signal processing for GNSS under ionospheric scintillation: Detection, monitoring, and mitigation. *Navigation: journal of the Institute of Navigation*, 67(3):511–536.

Zhao, W. and Pervan, B. (2019). IMM Methods for carrier phase tracking and navigation Data bits estimation through interference. *Proceedings of the 2019 International Technical Meeting of The Institute of Navigation*.

Zhao, W. and Pervan, B. (2020a). Data Bit assisted adaptive IMM filter for carrier phase tracking through interference. *Proceedings of the 33rd International Technical Meeting of the Satellite Division of The Institute of Navigation (ION GNSS+ 2020)*.

Zhao, W. and Pervan, B. (2020b). Experimental validation of IMM algorithm for carrier phase tracking through interference. *Proceedings of the 2020 International Technical Meeting of The Institute of Navigation*.